

# NMR Analysis of Oxidatively Aged HTPB/IPDI Polyurethane Rubber: Degradation Products, Dynamics, and Heterogeneity

D. J. Harris,\* R. A. Assink, and M. Celina

Sandia National Laboratories, Albuquerque, New Mexico 87185-1411

Received May 21, 2001

**ABSTRACT:** NMR spectroscopy experiments on thermally aged cross-linked hydroxyl-terminated polybutadiene (HTPB)/isophorone diisocyanate (IPDI) based polyurethane rubber indicated only a slight temperature dependence for the degradation products distribution but revealed the presence of chemical and dynamic heterogeneities. The samples were aged in sealed ampules containing either oxygen or  $^{17}\text{O}_2$  gas at temperatures ranging from ambient temperature to 125 °C. The  $^{17}\text{O}$  and  $^{13}\text{C}$  NMR spectra showed that alcohols are the dominant oxygen-containing degradation products (~60%). Ester and acid functional groups were also detected, but there was no significant amount of ketones. Gel permeation chromatography (GPC) showed evidence of both chain scission and cross-linking during degradation. The dynamics in the rubber system was probed with wide-line  $^1\text{H}$  spectra,  $^1\text{H}$  spin diffusion measurements, and 2D wide-line-separation (WISE) experiments. Dynamic and chemical heterogeneities were detected in highly aged materials. The smallest dimension of the chemically pristine mobile regions is ~20 nm.

## Introduction

Hydroxyl-terminated polybutadiene (HTPB)/isophorone diisocyanate (IPDI) based polyurethane rubber is used as a polymeric binder in solid propellants. Oxidative aging for many years results in brittle materials. Accelerated aging at elevated temperatures has been used to predict the lifetimes of this material.<sup>1</sup> The combination of ultrasensitive oxygen consumption measurements at ambient and high temperatures and mechanical testing at elevated temperature allows for accurate lifetime predictions if mechanical behavior is related to the extent of oxidation. The degradation mechanisms and products must be temperature-invariant to perform the correlation.<sup>2</sup> Non-Arrhenius behavior, possibly due to changing product distributions, has been reported for this polyurethane rubber. Observation of temperature-dependent degradation chemistry would demand reexamination of the predicted lifetime and thus was the focus of this work.

Previous studies have qualitatively characterized the degradation products for HTPB and polybutadiene. An FT-IR study of the oxidation of polybutadiene<sup>3</sup> has suggested the formation of hydroperoxides and/or alcohols and ketones. HTPB binder has also been studied by FT-IR spectroscopy,<sup>4</sup> and the spectra revealed the presence of degradation products with alcohol functionalities. An IR peak with a frequency of  $1698\text{ cm}^{-1}$  was present in the spectrum and seen as indicating unspecified types of carbonyl groups. Finally, the authors reported the loss of unsaturation. Neither of the FT-IR studies was quantitative or examined temperature dependencies of degradation.

The objective of this paper is to quantitatively determine the temperature dependence of HTPB oxidation products for unstabilized and antioxidant (AO) stabilized HTPB binder using both  $^{17}\text{O}$  and  $^{13}\text{C}$  NMR techniques. Evidence of cross-linking and scission were examined with gel permeation chromatography (GPC).

Additionally, dynamic and chemical heterogeneities were probed with  $^1\text{H}$  spin diffusion with cross polarization (CP) to  $^{13}\text{C}$  and 2D wide-line-separation (WISE) experiments.<sup>5–8</sup>

## Experimental Section

**Materials.** The polyurethane rubber is composed of HTPB cured with IPDI. Elf Atochem and Hüls America Inc. supplied the resins. The approximate functionality of the HTPB is 2.1, and the average molecular weight is  $M_n \approx 2800\text{ g/mol}$ . A ratio of HTPB to IPDI of 12.1:1 wt/wt was used to obtain an equal molar reactivity ratio. Samples for the  $^{13}\text{C}$  NMR aging study contained 1% Vanox MBPC antioxidant (2,2'-methylene-bis-(4-methyl-6-*tert*-butylphenol)). To determine the effects of antioxidant and to facilitate investigations of a wider aging temperature range, some samples used for  $^{17}\text{O}$  NMR spectroscopy were not stabilized. Resins were thermally cured in Teflon-coated molds for 1 week at 65 °C to obtain sheets of 2-mm thickness.

**Thermal Aging and Oxygen Consumption (Uptake).** Sheets were cut into shreds approximately 1 mm thick and placed in sealed steel ampules of known volume. The high relative surface areas of the samples were necessary to obtain more homogeneous degradation.<sup>1</sup> Calculations based on measured oxidation rates and permeability data were used to ensure that the degradation was not affected by diffusion-limited oxidation. The ampules were evacuated and refilled with 81% enriched  $^{17}\text{O}_2$  (Isotec) (or standard  $\text{O}_2$  gas for the  $^{13}\text{C}$  NMR experiments) to a pressure calculated to result in 150 mmHg at the relevant aging temperature. The containers were then placed in temperature-controlled ( $\pm 1\text{ }^\circ\text{C}$  stability) commercial air-circulating aging ovens. The aging times were calculated to allow for approximately 30% of the oxygen to be consumed, thus resulting in an average partial pressure during each aging exposure equal to the ambient air conditions in Albuquerque, NM, 130 mmHg. Varying the ratio of sample to gas volume in the sealed ampules and the aging time determined the overall oxidation level of the sample and resulted in a sensitivity range for oxidation rate of  $10^{-13}$ – $10^{-8}\text{ mol O}_2\text{ g}(\text{sample})^{-1}\text{ s}^{-1}$ .<sup>2,9</sup> The consumption of  $\text{O}_2$  and generation of  $\text{CO}_2$  and CO during aging was monitored by gas chromatography (GC). A summary of samples used for the  $^{17}\text{O}$  oxidation studies is listed in Table 1. The amount of generated  $\text{CO}_2$  typically increases with aging temperature, although scatter in the data partially masks this expected result. The absence of water and small-molecule analysis is a current deficiency in the oxygen

\* Contact information: Douglas J. Harris, Sandia National Laboratories, Albuquerque, NM 87185-1411. Phone number: (505) 844–9511. Fax number: (505) 844–9781. E-mail: djharri@sandia.gov.

**Table 1. Oxygen Uptake Measurements on HTPB/IPDI Binder Samples Used for the  $^{17}\text{O}$  NMR Studies**

sample <sup>a</sup>	exposure	O <sub>2</sub> in sample (wt %)	CO <sub>2</sub> (%)	CO (%)
HTPB + 1% AO	10 days at 110 °C	1.89	18	3
HTPB + 1% AO	60 days at 95 °C	2.04	23	3
HTPB + 1% AO	256 days at 80 °C	1.38	32	2
HTPB + 1% AO	180 days at 80 °C	1.19	21	2
HTPB + 1% AO	575 days at 65 °C	0.62	19	2
HTPB, no AO	2.25 days at 80 °C	3.27	19	2
HTPB, no AO	14 days at 50 °C	3.87	14	1
HTPB, no AO	38 days at 37 °C	4.11	12	1
HTPB, no AO	145 days at 23 °C	3.68	6	3

<sup>a</sup> Some samples contain Vanox MBPC antioxidant (AO). The exposure times were estimated to allow approximately constant oxidation levels. The amounts of liberated CO<sub>2</sub> and CO gases are calculated as percentages of consumed O<sub>2</sub>. The column for O<sub>2</sub> in sample might overestimate the true value as a result of neglect of generated H<sub>2</sub>O.

consumption technique.<sup>10</sup> Water in the sample was detected in the  $^{17}\text{O}$  spectra, but the headspace concentration was not quantified.

**GPC.** Aged samples were extracted in refluxing tetrahydrofuran (THF) for 24 h. The soluble fractions, with polymer concentrations of ~5 mg/mL, were analyzed on a Waters Alliance GPCV2000 instrument. The column set consists of a bank of six columns manufactured by Polymer Labs. The particle size was 5  $\mu\text{m}$  and the pore types are 50, 100, 500, 1000, 10 000, and 100 000 Å. The instrument conditions were THF with a flow rate of 1.0 mL/min at a temperature of 40 °C. The injection volume was 206  $\mu\text{L}$ . The molecular weight was calibrated using polybutadiene standards.

**$^{17}\text{O}$  NMR Spectroscopy.** The  $^{17}\text{O}$  NMR spectra were obtained on a Bruker DRX400 NMR spectrometer at a resonant frequency of 54.3 MHz using a 5-mm broadband probe. The oxidized samples were swollen in hot 1,2,4-trichlorobenzene (Aldrich) to decrease the molecular correlation time and thus reduce the observed line widths in the NMR spectra.<sup>11</sup> Approximately 0.1 g of each sample and 0.5 mL of trichlorobenzene were placed in 5-mm NMR tubes. The spectra were collected at 75 °C with quadrupolar spin-echo and proton decoupling using the following parameters: 90° pulse length = 11  $\mu\text{s}$ , spin-echo delay = 10  $\mu\text{s}$ , recycle delay = 0.2 s, dwell time = 7.7  $\mu\text{s}$ , acquisition time = 15 ms, number of scans = 200k, total experiment time  $\approx$  12 h. The spectra were calibrated to an external H<sub>2</sub>O standard at 25 °C, which has a sharp peak assigned to  $\delta = 0$  ppm.

**$^{13}\text{C}$  NMR Spectroscopy.** The  $^{13}\text{C}$  NMR spectra were obtained on a Bruker AMX400 spectrometer with a  $^1\text{H}$  frequency of 400.2 MHz and a  $^{13}\text{C}$  frequency of 100.6 MHz. Aged and unaged binder samples were packed in 4-mm-diameter zirconia rotors, and spectra were obtained under magic-angle spinning (MAS) conditions. Typical 90° pulse lengths for  $^{13}\text{C}$  and  $^1\text{H}$  were 4.0 and 3.9  $\mu\text{s}$ , respectively. Hahn echoes were used in all experiments to minimize baseline distortions. Quantitative  $^{13}\text{C}$  spectra were obtained with direct-polarization excitation (single  $\pi/2$  pulse), a 10-kHz spinning speed, and a 7-s recycle delay. The  $^1\text{H}$  decoupling field strength for all experiments was 80 kHz. The chemical shifts were calibrated to an external glycine reference with the carbonyl peak assigned to  $\delta = 176.0$  ppm.

**$^1\text{H}$  NMR Spectroscopy.**  $^1\text{H}$  NMR spectra were recorded on the Bruker AMX400 spectrometer. Samples were placed in 4-mm rotors and spun at 1 kHz to narrow the peaks from mobile components but leave rigid lines unmodified. The repetition time for all experiments was 5 s, and the number of scans was 128. The dwell time was set to 1  $\mu\text{s}$ , but because of pulse ring-down problems, the effective dead time was 8  $\mu\text{s}$ . The loss of initial signal results in the reduction of broad-component intensities, and the spectra are not quantitative. A background spectrum obtained using an empty rotor was recorded using identical experimental conditions and subtracted from each spectrum.

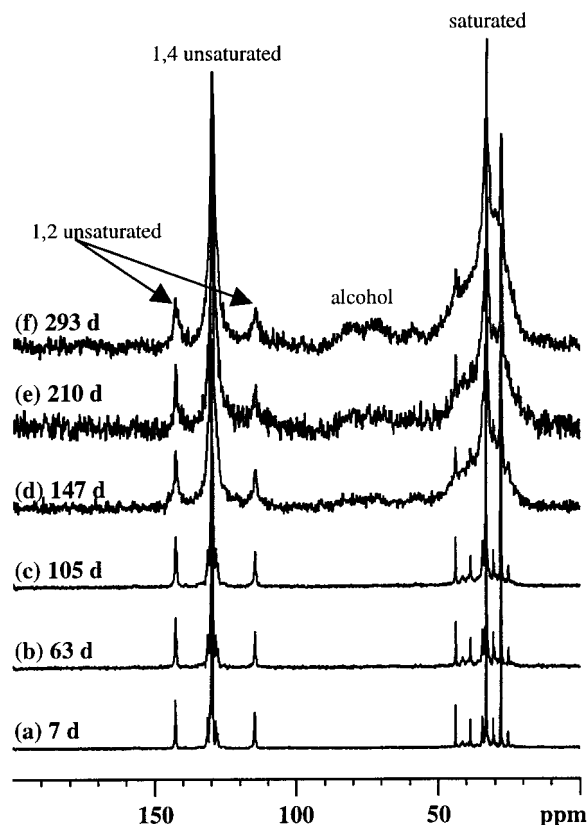


**Figure 1.** Solid-state  $^{13}\text{C}$  direct-polarization spectra under MAS conditions of HTPB/IPDI polyurethane aged at 80 °C for (a) 7, (b) 63, (c) 105, (d) 147, (e) 210, and (f) 293 days. All spectra are scaled to the same height.

**Spin Diffusion Experiments.**  $^1\text{H}$  spin diffusion<sup>8,12–14</sup> techniques were used to elucidate the morphology of the aged HTPB binder. A Goldman–Shen experiment<sup>15</sup> was performed with a 40- $\mu\text{s}$  delay to dephase the rigid component. The remaining magnetization was stored in the  $\pm z$  directions during the spin diffusion mixing time, which ranged between 0.1 and 243 ms. A 90°  $^1\text{H}$  pulse returned the magnetization to the  $xy$  plane. Finally, the magnetization was transferred to  $^{13}\text{C}$  nuclei using a 1-ms CP contact time. For each spin diffusion mixing time, the number of scans was 2048, and the recycle delay was 2 s. The decay of signal due to  $T_1$  relaxation during the mixing time was corrected by running a series of experiments with a short (2- $\mu\text{s}$ ) dephasing time and with mixing times corresponding to the values used in the spin diffusion experiments.<sup>8,16</sup> All samples were spun at 4 kHz.

**2D WISE Experiments with  $^1\text{H}$  Spin Diffusion.** Heterogeneity in dynamics was also investigated using 2D WISE experiments<sup>5–8</sup> with short and long  $^1\text{H}$  spin diffusion mixing times. The two mixing times were 0.1 and 100 ms. In the  $t_1$  dimension, 64 slices with increments of 5  $\mu\text{s}$  were acquired. The CP and signal acquisition times were 1 and 10 ms, respectively. Each slice was the sum of 512 scans, and the total experiment time for each spectrum was 12 h. The samples were spun at 4 kHz.

## Results and Discussion

**Degradation Products.** The combination of  $^{13}\text{C}$  and  $^{17}\text{O}$  NMR spectroscopy allowed for quantitative determination of new functional groups generated from oxidative degradation. Solid-state  $^{13}\text{C}$  NMR experiments under MAS conditions recorded the disappearance of unsaturated functional groups and the creation of alcohol and saturated species. Spectra of samples containing antioxidant and aged at 80 °C are shown in Figure 1. The spectrum of relatively unaged rubber (7

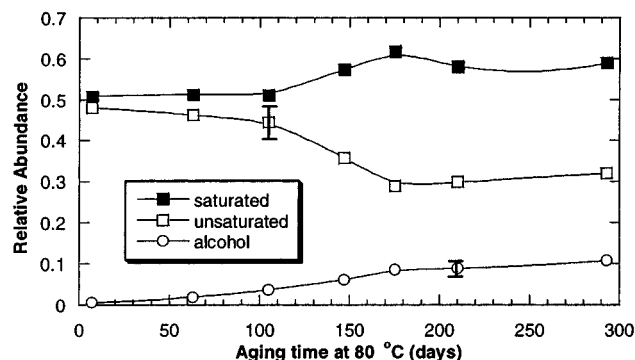


**Figure 2.** Relative abundance plot of functional groups obtained from the  $^{13}\text{C}$  NMR spectra. Lines are guides for the eye.

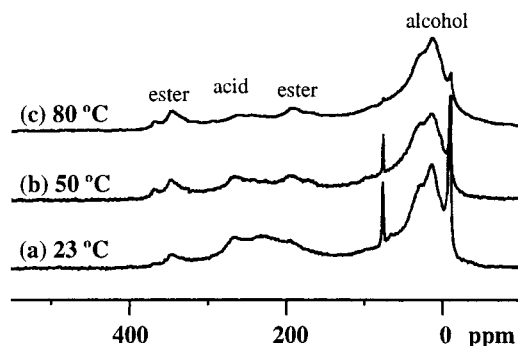


**Figure 3.** Solution  $^{17}\text{O}$  NMR spectrum of polyurethane with no antioxidant aged for (a) 145 days at 23 °C, (b) 14 days at 50 °C, and (c) 2.25 days at 80 °C. All spectra were obtained in trichlorobenzene at 75 °C. The  $^{17}\text{O}$  abundance in these samples is approximately 3.5 wt % (see Table 1).

days at 80 °C) shows that initially half of the carbons, as expected for polybutadiene, are unsaturated hydrocarbons. The distribution of this unsaturation is calculated from the integration of the discernible peaks: 22% 1,2-unsaturation ( $\delta = 114.7$  and 142.6 ppm), 55% trans 1,4-unsaturation ( $\delta = 130.2$  ppm), and 23% cis 1,4-unsaturation ( $\delta = 130.0$  ppm). These ratios are expected from information provided by the manufacturer. After aging, the peaks broaden, a lower percentage of carbons is unsaturated, and both alcohol and carbonyl degradation products appear. The peak arising from the alcohols is broad, ranging from 65 to 85 ppm. This breadth might be the result of the combination of primary, secondary, and tertiary functional groups. Diols might also be responsible for the high chemical shift of some  $^{13}\text{C}$  nuclei. Integration of the regions yielded the relative abundance of saturated, unsaturated, and alcohol groups. A graph of the results (Figure 2) shows that oxidative degradation of the unsaturated carbons results in an approximately equal increases in both alcohols and saturated aliphatics. Small peaks in the carbonyl region were observed in  $^{13}\text{C}$  cross-polarization spectra but were not quantified.

The  $^{17}\text{O}$  NMR spectra of aged HTPB binders provide complimentary information on the degradation products. Spectra of aged materials without antioxidants are shown in Figure 3. The observed peaks were assigned to degradation products on the basis of small model compounds<sup>17</sup> and oxidized polymers.<sup>10,11</sup> The main peak is observed at  $\delta = 11$  ppm in all spectra. Primary, secondary, and tertiary alcohols have typical  $^{17}\text{O}$  chemical shifts of  $\delta \approx 0$ , 35, and 60 ppm, respectively. Therefore, the principal  $^{17}\text{O}$  peak is assigned to primary

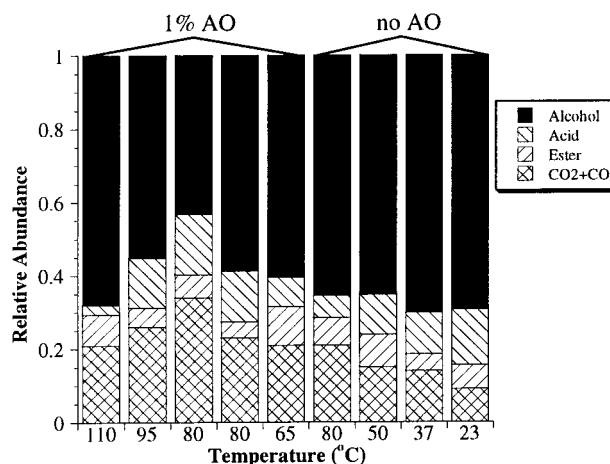


**Figure 4.** Degradation products derived from  $^{17}\text{O}$  NMR and GC analyses of HTPB/IPDI polyurethane rubbers containing 1% antioxidant (left) and no antioxidant (right). The relative abundance of alcohol functional groups shows little systematic trends with aging temperature or presence of antioxidant.

alcohols, and the broad shoulders on the left side indicate the presence of higher-order and/or unsaturated alcohol groups. Two sharp components are also observed in the alcohol region. The right component at  $\delta = -9.2$  ppm is attributed to  $\text{H}_2\text{O}$ , but the peak at 77.3 ppm is an unidentified small molecule. These compounds are not observed in the neat solvent and must be byproducts of the oxidative degradation. The presence of degradation products containing hydroxyl functionalities is consistent with the previous FT-IR reports.<sup>3,4</sup>

In addition to alcohols, carbonyls are seen in all spectra. Ester functional groups result in two observed peak regions at  $\delta = 350$  and 195 ppm that correspond to the  $\text{C}=\text{O}$  and  $\text{C}-\text{OR}$  oxygens, respectively. Two distinguishable types of ester degradation products result in the four identifiable peaks, but we have not attempted to assign these resonances to specific structures. Carboxylic acids are also present in the spectra. Because of exchange of the attached hydrogen, both oxygen atoms are observed as a single peak at 260 ppm. The intensity of the acid peak decreases with aging temperature. This disappearance is attributed to the high-temperature conversion to  $\text{CO}_2$  gas as detected in the GC analyses summarized in Table 1.

A bar graph of oxygen-containing degradation products, calculated from the  $^{17}\text{O}$  peak integrals and GC data, is shown in Figure 4. The area of the ester peaks is calculated from the more resolved downfield peaks. Subtraction of the ester area from the carbonyl region yields the estimated acid fraction. The areas of the carbonyl peaks are then divided by 2, the number of oxygens per functional group. The results of the calculations are consistent with the  $^{13}\text{C}$  NMR spectra: alcohols are the major degradation products. The total quantity of carbonyl functional groups and released  $\text{CO}_2$  has an average value of 40% of the consumed  $\text{O}_2$ . There might be an overall trend of increased liberation of  $\text{CO}_2$  and  $\text{CO}$  gas at higher temperature and, thus, lower concentrations of remaining carboxylic acids and ester species in the aged materials. A more thorough investigation of the temperature dependence of liberated gases is currently being conducted on a variety of materials.

The observation of primary alcohols and carboxylic acids leads to interesting conclusions: the relative abundance of these functional groups exceeds the loss



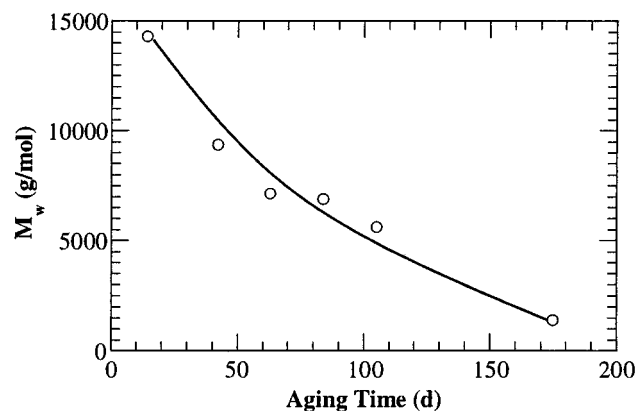


**Figure 5.** GPC-determined weight-averaged molecular weights of extractable chains in materials aged at 80 °C. The line is guidance for the eye and does not represent a fit.

of 1,2-butadiene units, indicating that the new functional groups cannot be purely isolated in the small side chains. The formation of primary alcohol and carboxylic acid functional groups from 1,4-butadiene units necessarily results in chain scission. However, the NMR spectra showed that oxidation of unsaturated carbons also creates saturated carbons. Other techniques suggest that most of the newly formed saturated carbons are cross-links. The gel content of materials was reported to increase from 60% for unaged samples to a plateau value of 90% after extensive degradation.<sup>1</sup> Additionally, the cross-link density of the gel component increases as seen in the decreased degree of swelling potential (solvent uptake factor reduction from 50 to 5) in refluxing *p*-xylene.<sup>1</sup> Information on the importance of chain scission was provided by GPC. The initial weight-average molecular weight,  $M_w$ , of the THF soluble fraction is 14 kg/mol, and the polydispersity index is approximately 2. After aging at 80 °C, the molecular weight of the extracted fraction decreases, as shown in Figure 5. After 175 days, the soluble chains are shorter with  $M_w = 1.4$  kg/mol. These short chains were not present in such abundance in unaged materials and must be caused by scission. The gel content, GPC, and NMR results are consistent with the hypothesis that oxidation leads to both chain cross-linking and scission, with a preponderance of the former.

#### Dynamics and Heterogeneity in Aged Rubber.

The polyurethane samples became stiffer and more brittle with aging. Wide-line  $^1\text{H}$  NMR spectra (Figure 6) illustrate the change of dynamics. Broad line widths indicate slow dynamics, whereas narrow lines are due to fast dynamics. The spectrum of unaged material contains two sharp peaks corresponding to protons attached to unsaturated and saturated carbons. The half-width at half-maximum (HWHM) broadens slightly from 62 to 100 Hz for samples aged between 14 and 100 days at 80 °C. A sudden change in dynamics was observed in the material aged 147 days. The  $^1\text{H}$  spectrum shows the appearance of a rigid component in addition to the continued presence of the more narrow peaks, now broadened to a HWHM of 500 Hz. Longer aging times resulted in an increase of the rigid component but no further broadening of the mobile component. The broad component is indicative of a rigid phase with dynamics limited by either increased cross-link density or higher levels of degradation. The broadening of the mobile component might be the result of slower dynamics due to close proximity with the rigid phase.<sup>18</sup>

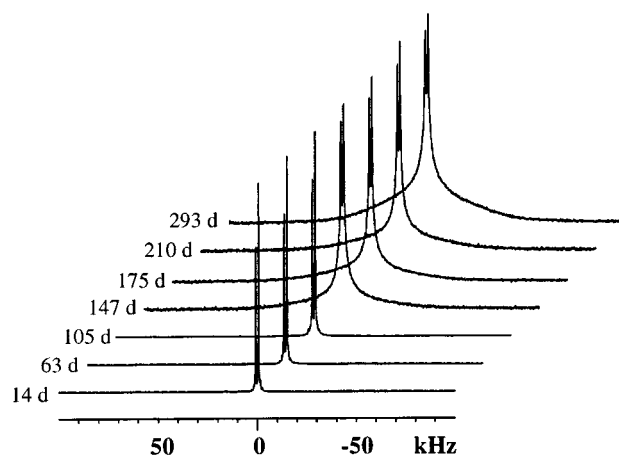


**Figure 6.**  $^1\text{H}$  wide-line NMR spectra of polyurethane rubbers aged at 80 °C. The two lines in the relatively pristine samples arise from the unsaturated and saturated functional groups. Rigid components appear in samples aged longer than 147 days.

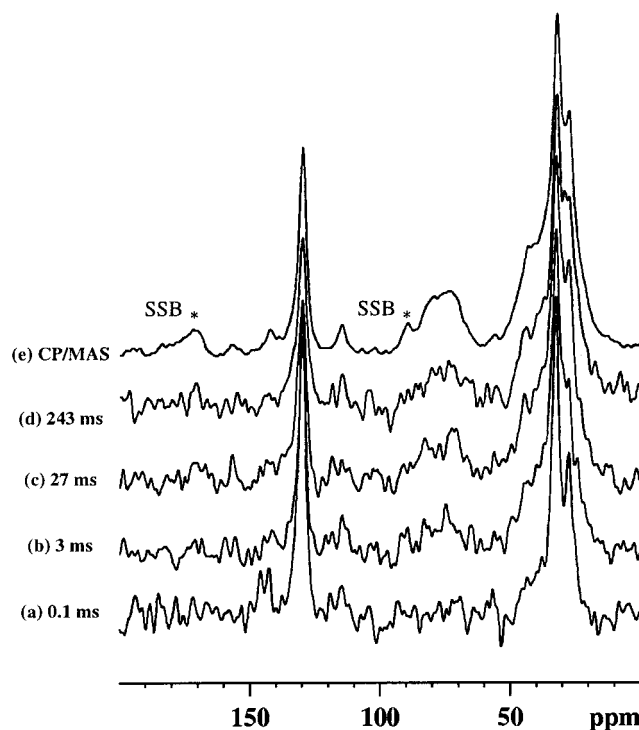


**Figure 7.** CP-detected  $^1\text{H}$  spin diffusion experiment. The  $^1\text{H}$   $T_2$  filter initially removes magnetization in the rigid domains. The  $^{13}\text{C}$  peak from alcohol functional groups ( $\delta = 75$  ppm) is initially absent but returns in spectra obtained with long mixing times. Two significant spinning sidebands are present in the spectra.

The length scales of the domains observed in the wide-line  $^1\text{H}$  spectra were investigated with  $^1\text{H}$  spin diffusion experiments detected via CP to  $^{13}\text{C}$ . A 40- $\mu\text{s}$  delay after initial excitation dephases the magnetization in the rigid component. A diffusion-like process transfers magnetization back to the rigid domains during the mixing time. Figure 7 shows a stack plot of  $^{13}\text{C}$  spectra obtained with various mixing times in an experiment using polyurethane aged 293 days at 80 °C. The mobile component contains little degradation product, and initially, the alcohol peak at  $\delta = 75$  ppm is absent. The spectra show that during the spin diffusion mixing time, magnetization is transferred to the dynamically rigid

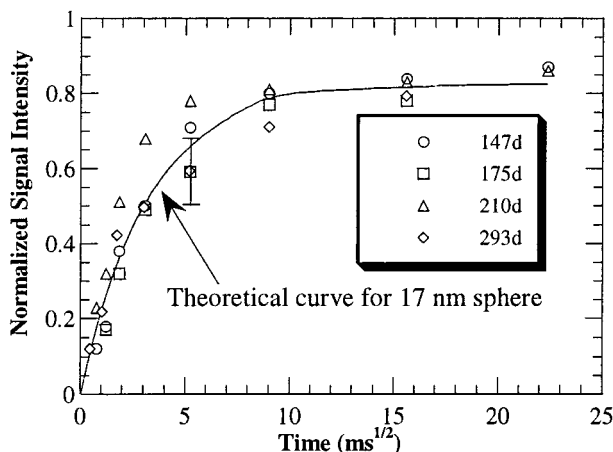


**Figure 8.** Dependence of alcohol peak intensity on spin diffusion mixing time. A theoretical curve is shown assuming 17-nm-diameter spheres. The curve estimates that 17% of the hard segments are in domains with long length scales ( $\geq 100$  nm).

components that contain the alcohol functional groups. After 243 ms, the magnetization has mostly, but not fully, equilibrated. At equilibrium, the spectrum should be identical to the simple  $^{13}\text{C}$  CP/MAS spectrum shown at the top of the figure.

The length scales of the chemical heterogeneities are estimated by the buildup curve of the alcohol peak, shown in Figure 8. Materials aged for 147, 175, 210, and 293 days all exhibited similar curves. The magnetization is nearly equilibrated after a mixing time of 81 ms. However, large heterogeneities are present as indicated by the incomplete return of intensity and slow change of the buildup curve at long mixing times. Quantification of the length scale relies on the effective spin diffusion coefficient that was estimated from the  $^1\text{H}$   $T_2$  relaxation constants measured under 4-kHz MAS conditions.<sup>12,19</sup> The effective diffusion coefficient was calculated to be  $0.6 \text{ nm}^2/\text{ms}$ . The line drawn in the graph represents the curve expected if the dispersed domains were 17-nm spheres.<sup>20</sup> We expect that the inhomogeneities have a three-dimensional geometry and thus chose spheres for the model. The curve assumes that 17% of the alcohol functional groups are in large domains with a length scale of 100 nm. The component with a large length scale is necessary to account for incomplete equilibration in spectra obtained with a mixing time of 500 ms. An initial rate approximation<sup>20</sup> for the spin diffusion curves yields a similar domain size, 20 nm, for the smallest dimension of the chemical heterogeneities. The many assumptions necessary to estimate the domain size result in a large uncertainty in the value. However, the magnitude can be used to reject many possible explanations for the origin, including surface effects.

Finally, heterogeneous dynamics was probed with 2D WISE experiments.<sup>7</sup> The spectra correlate the wide-line  $^1\text{H}$  spectra with the isotropic  $^{13}\text{C}$  chemical shifts of nearby carbons. The 2D spectrum in Figure 9a shows that the unsaturated functional groups at  $\delta = 130$  ppm have fast dynamics (narrow  $^1\text{H}$  cross section) and the alcohols at  $\delta = 75$  ppm are rigid (broad  $^1\text{H}$  cross section). Saturated carbons have a mixture of fast and slow dynamics, as observed by the two distinct line shapes in the  $\delta = 32$  ppm cross section. During a 100-ms  $^1\text{H}$  spin diffusion mixing time prior to CP, the magnetization readily transfers from the mobile regions to the

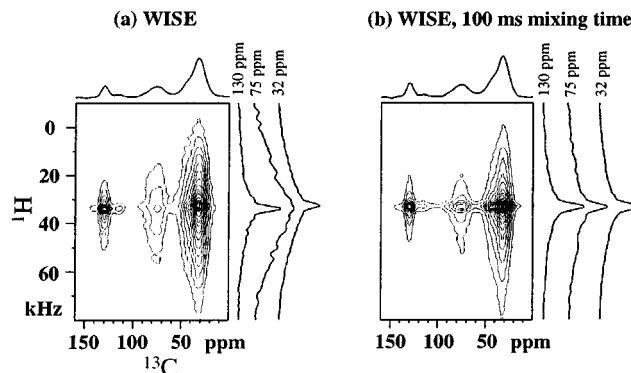


**Figure 9.** 2D WISE spectra obtained with (a) 0.1- and (b) 100-ms spin diffusion mixing times.

rigid domains, as shown from the 2D spectrum in Figure 9b. The cross sections for the unsaturated, alcohol, and saturated functional groups all have the same narrow line shape. This result is complementary to the information revealed by the  $^1\text{H}$  spin diffusion experiments and shows that the smallest dimensions of chemical and dynamic inhomogeneities are both on the length scale of  $\sim 20$  nm.

The observation of nearly pristine, yet very small, domains dispersed throughout the highly aged rubber is an unusual discovery. Diffusion-limited oxidation or volatilization of antioxidants might explain the small fraction of very large heterogeneities, but they cannot be factors leading to the  $\sim 20$ -nm regions. These effects are typically important on the millimeter and centimeter length scales, and the small molecules can readily equilibrate in the very small domains observed in this work. The calculated length scale is too large to be explained by a simple stochastic distribution of degradation products where parts of the chain will randomly have above- or below-average oxidation levels. One possible theory is the presence of a higher antioxidant concentration in the undegraded regions due to either preferential solubility of the hindered phenol molecules or creation of antioxidants by oxidative degradation. The oxidative degradation products have been reported to be pro-oxidants,<sup>1</sup> so the latter is unlikely, but not impossible.

## Conclusions

The various techniques used in this paper lead to consistent conclusions. Aging of the HTPBI/IPDI polyurethane results in the formation of alcohols, carboxylic acids, and esters. The degradation results in both chain cross-linking and scission. Approximately 60% of the oxidation products are alcohols, independent of temperature and the presence or absence of antioxidants. The remaining oxidative products are principally acids, esters, and  $\text{CO}_2$ . The invariance in product distribution supports the validity of mechanical property extrapolation to ambient temperatures on the basis of oxygen uptake measurements.

This work also characterized the slower chain dynamics in the degraded samples. The NMR spectra showed that the degree of degradation is not homogeneous.  $^1\text{H}$  NMR spectra revealed both broad and narrow components in highly aged rubbers. Spin diffusion and 2D WISE experiments indicated that the alcohol degradation products are only present in the rigid domains. The length scale of the heterogeneity is approximately 20 nm for the smallest dimension and is aging-temperature

invariant. More research is necessary to address the origin of the heterogeneity.

**Acknowledgment.** Sandia is a multiprogram laboratory operated by Sandia Corporation, a Lockheed Martin Company, for the United States Department of Energy under Contract DE-AC04-94AL8500. Special thanks go to Bertha M. Montoya for GPC analysis and to Leanna Minier for her ideas.

## References and Notes

- (1) Celina, M.; Graham, A. C.; Gillen, K. T.; Assink, R. A.; Minier, L. M. *Rubber Chem. Technol.* **2000**, *73*, 678.
- (2) Gillen, K. T.; Celina, M.; Clough, R. L.; Wise, J. *Trends Polym. Sci.* **1997**, *5*, 250.
- (3) Földes, E.; Lohmeijer, J. *Polym. Degrad. Stab.* **1999**, *66*, 31.
- (4) Ahlblad, G.; Reitberger, T.; Terselius, B.; Stenberg, B. *Polym. Degrad. Stab.* **1999**, *65*, 185.
- (5) Zumbulyadis, N. *Phys. Rev. B* **1986**, *33*, 6495.
- (6) Tekely, P.; Nicole, D.; Brondeau, J.; Delpuech, J. J. *J. Phys. Chem.* **1986**, *90*, 5608.
- (7) Schmidt-Rohr, K.; Clauss, J.; Spiess, H. W. *Macromolecules* **1992**, *25*, 3273.
- (8) Schmidt-Rohr, K.; Spiess, H. W. *Multidimensional Solid-State NMR and Polymers*; Academic Press: New York, 1994.
- (9) Wise, J.; Gillen, K. T.; Clough, R. L. *Polym. Degrad. Stab.* **1995**, *49*, 403.
- (10) Alam, T. M.; Celina, M.; Assink, R. A.; Clough, R. L.; Gillen, K. T.; Wheeler, D. R. *Macromolecules* **2000**, *33*, 1181.
- (11) Alam, T. M.; Celina, M.; Wheeler, D. R.; Assink, R. A.; Clough, R. L. *Polym. News* **1999**, *24*, 186.
- (12) Mellinger, F.; Wilhelm, M.; Spiess, H. W. *Macromolecules* **1999**, *32*, 4686.
- (13) VanderHart, D. L.; McFadden, G. B. *Solid State Nucl. Magn. Reson.* **1996**, *45*.
- (14) VanderHart, D. L. *Makromol. Chem. Macromol. Symp.* **1990**, *34*, 125.
- (15) Goldman, M.; Shen, L. *Phys. Rev.* **1966**, *144*, 321.
- (16) Packer, K. J.; Pope, J. M.; Yeung, R. R.; Cudby, M. E. A. *J. Polym. Sci. B: Polym. Phys.* **1984**, *22*, 589.
- (17) Chandrasekaren, S.; Boykin, D. W.; Baumstark, A. L. *<sup>17</sup>O NMR Spectroscopy in Organic Chemistry*; CRC Press: Boca Raton, FL, 1991.
- (18) Harris, D. J.; Bonagamba, T. J.; Schmidt-Rohr, K.; Soo, P.; Sadoway, D. R.; Mayes, A. M. *Macromolecules* **2001**, in press.
- (19) Demco, D. E.; Johansson, A.; Tegenfeldt, J. *Solid State Nucl. Magn. Reson.* **1995**, *4*, 13.
- (20) Clauss, J.; Schmidt-Rohr, K.; Spiess, H. W. *Acta Polym.* **1993**, *44*, 1.

MA0108766